NANO LETTERS

2008
Vol. 8, No. 4
1229-1236

MspA Porin−Gold Nanoparticle Assemblies: Enhanced Binding through a Controlled Cysteine Mutation

Raj Kumar Dani, Myungshim Kang, Mausam Kalita, Paul E. Smith, Stefan H. Bossmann, and Viktor Chikan*

Department of Chemistry, Kansas State University, Manhattan, Kansas 66506-3701

Received October 15, 2007; Revised Manuscript Received February 13, 2008

ABSTRACT

In this study, the interactions of two gold nanoparticles of different sizes (average diameters of 3.7 ± 2.6 and 17 ± 3 nm) with octameric mycobacterial porin A from *Mycobacterium smegmatis* (MspA) and a mutant of MspA featuring a cysteine mutation in position 126 (Q126C) are investigated. From the observation of enhanced photoluminescence quenching, it is inferred that the presence of eight cysteines in the MspA Q126C mutant significantly enhances the binding of selected small gold nanoparticles within the inner pore of MspA. The large gold nanoparticle/porin complex shows photoluminescence enhancement, which is expected since the larger nanoparticles cannot dock within the homopore of MspA due to size exclusion. In addition to the fluorescence experiments, observation of energy transfer from the small gold nanoparticles to the MspA shows the close proximity of the small gold nanoparticles with the porin. Interestingly, the energy transfer of the large nanoparticle/MspA complex is completely missing. From high-performance liquid chromatography data, the estimated binding constants for small Au@MspA, large Au@MspA, small Au@MspA^{cys}, and large Au@MspA^{cys} are 1.3 × 10^9, 2.22 × 10^{10}, > 10^{12} (irreversible), and 1.7 × 10^{10}, respectively.

Proteins are macromolecules with dimensions in the nanometer range that can be tailored to specific needs by site-directed mutagenesis. Combining nanoparticles with proteins is desirable to extend the functionality and transferability of both proteins and nanoparticles. Nanoparticles have been successfully linked to antibodies,[1,2] aptamers,[3,4] and enzymes.[5,6] Extensive work has been done creating nanoparticle/biomacromolecule complexes by many groups,[7–9] but challenges remain. Specifically, using protein/nanoparticle complexes has been severely hampered by the problem that most proteins lose their structural integrity in a non-native environment, limiting their potential use in many analytical and clinical procedures.[10]

The octameric porin A from *Mycobacterium smegmatis* (MspA) forms a homopore, which distinguishes itself by its extraordinary stability, suitable geometric dimensions, and an amphiphilic nature. This porin features a very hydrophobic docking unit that is able to penetrate virtually any cell membrane. When MspA is doped with a nanoparticle (NP) of suitable dimensions (<5 nm in diameter), the resulting nanoparticle@MspA assembly will reconstitute within virtually all human (mammalian) cell membranes using the strongly hydrophobic "docking region" (see Figure 1). The geometric dimensions of this docking region are 3.7 nm in length and 4.9 nm in diameter.[11] In sharp contrast, the inner pore of MspA is hydrophilic. The diameter of the inner pore changes from 4.8 nm at the pore's entrance to 1.0 nm at its constriction zone (bottleneck). Due to the strong binding of hydrophilic functional groups to the surface of gold (and other metal) nanoparticles, the inner pore can act as host for nanoparticles of suitable size. In order to test the potential of this porin to dock nanoparticles, two different sizes of gold nanoparticles are synthesized. Thiols are known to bind most strongly to gold surfaces and to competitively displace other functional groups, such as amines and carboxylates. Therefore, the effect of a cysteine mutant of MspA (Q126C,

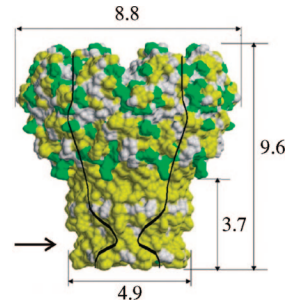

Figure 1. Crystal structure of MspA.[8] Surface representation (side view): green, hydrophilic amino acids; yellow, hydrophobic amino acids. Dimensions are given in nanometers. The position of the constriction zone (d = 1 nm) is marked with an arrow. The inner channel lining is indicated by black lines.

* Author to whom all correspondence should be addressed. E-mail: chikan@ksu.edu.

10.1021/nl072658h CCC: $40.75
Published on Web 03/05/2008

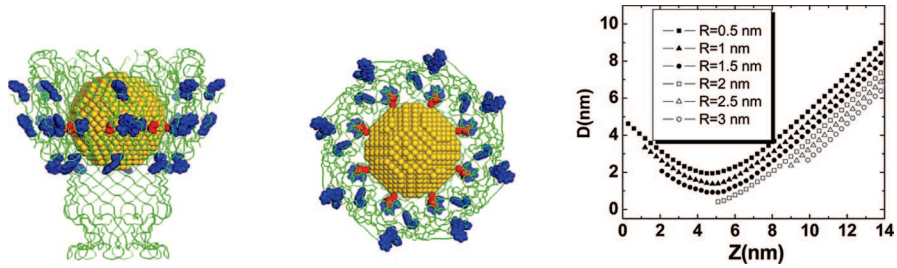

Figure 2. (a) The optimal arrangement for a nanoparticle of radius 2 nm. The closest S−Au distance is 0.42 nm. Gray represents the C^{α} backbone, gold the Au sphere, blue the Trp, and red the Cys 126. (b) The distance (D) of the nearest Au atom of the nanoparticle to the C^{β} of residue 126 as a function of distance from the base of the porin (Z) along the central axis of the porin. The origin ($Z = 0$) is defined by the C^{α} position of each D91 residue. The lines correspond to spherical Au nanoparticles of varying radius (R), and the horizontal line is the optimal C^{β}−Au distance (0.33 nm) required for S−Au bond formation (0.24 nm). Curves are truncated when an Au atom is located within 0.3 nm of a backbone or C^{β} atom of the porin (steric overlap). An optimal arrangement is observed for a nanoparticle of radius 2 nm (containing 1956 atoms) located at $Z = 5.1$ nm with a C^{β}−Au distance of $D = 0.42$ nm.

henceforth abbreviated as $MspA^{cys}$) is also investigated on the binding of gold nanoparticles.

Our Au@MspA adducts are intended for plasmonic hyperthermia[12] experiments and serve as model compounds for magnetic hyperthermia experiments.[2] Compared to other methods for treating cancer, such as chemotherapy and radiation, hyperthermia has profound advantages: (A) When heated above 45 °C, mammalian cells die because of protein misfolding, impairing DNA transcription, and many other metabolic functions.[13] Furthermore, the kinetic energy of the phospholipids in the cell membrane can exceed the hydration energy barrier, which holds them within the supramolecular assembly of the membrane. The membrane of mammalian cells at 43 °C dissolves in the surrounding aqueous buffers, rendering the membrane freely permeable to small ions. This process leads to either necrosis (leakage of the cell components in the human body) or apoptosis, depending on the amount of ion influx into the cytoplasm and the efficacy of the cellular repair mechanisms, which can be also impaired by hyperthermia.[14] (B) Heat is not toxic and will not destroy too many healthy cells, if the heating can be restricted to the tumor region(s) with precision. With nanoparticles, heating can be either induced by multiphotoabsorption at 800 nm,[15] where human tissue is almost transparent and does not scatter significantly,[16] or by the application of a local AC field when magnetic nanoparticles are used.

MspA Porin/Gold Complex. Nanoparticle/protein complexes represent a unique class of materials that are able to increase the functionality of the individual components. We have assessed the ability of the very stable porin (MspA) from *M. smegmatis* to bind two very differently sized gold nanoparticles in the hydrophilic inner pore. The binding of the gold nanoparticles has been probed by observing the fluorescence and phosphorescence of tryptophan molecules positioned in the protein (Figure 2a). MspA contains eight identical amino acid chains. Each MspA chain is composed of 184 amino acid residues and contains four tryptophan fluorophores at positions 21, 40, 72, and 181. The positions of the 32 tryptophans of the MspA are shown in Figure 2a.

In order to determine the geometrical requirements for the formation of a gold nanoparticle and MspA complex (Au@MspA) a series of calculations are performed using the porin octamer coordinates obtained from the crystal structure (PDB code: 1UUN). Figure 2 predicts that the optimal size for the complex formation involves a nanoparticle with a diameter of 4 nm. A larger diameter will not fit into the porin, while a smaller diameter will not be able to covalently attach to all eight C126 residues simultaneously. Smaller Au clusters could enter and bind asymmetrically—although their ability to totally block the porin would be reduced substantially. The figure also suggests that a 4 nm diameter Au nanoparticle should form a complex with its center approximately 5.1 nm away from the constriction zone and with Au atoms within 0.42 nm of the C^{β} of residue 126. While this is slightly larger than the optimal distance of 0.33 nm (see Methods), covalent attachment can easily be accommodated by small, but benign, changes in the porin structure. The covalent attachment to C126 is predicted to occur around the equator of the nanoparticle. Finally, we note that in the above complex the closest tryptophan to Au distances are approximately 2.5, 1.1, 1.4, and 2.0 nm for residues 21, 40, 72, and 181, respectively.

The transmission electron microscope images of these two samples are shown in Figure 3. The size histograms of the gold nanoparticles are also presented in the figure. The average sizes are 3.7 ± 2.6 and 17 ± 3 nm. The respective sizes of the gold nanoparticles used in our experiments are both smaller and larger than the channel opening of MspA, which is 4.8 nm. It is apparent from these data that the larger gold nanoparticles are unable to fit into channel opening or even the outer pore of MspA. However, the sample of smaller gold nanoparticles feature a significant fraction that is less than 4.8 nm in diameter. Fortunately, nanoparticles with diameters of 4.0 nm correspond to the most common particle size synthesized for the small Au clusters. Our experiments are based on the mechanistic paradigm that the smaller gold nanoparticles are in close proximity to the tryptophan side chains at positions 21, 40, 72, and 181. Hence, this will result in different spectral features than for larger nanoparticles which have to remain outside of the central pore of MspA.

Stationary luminescence experiments of the Au@MspA complexes have been performed. The goal of these experiments is to confirm the presence of Au@MspA complexes when using smaller nanoparticles and to discern the effect of the various sized gold nanoparticles on the tryptophan emission. Furthermore, the effect of the cysteine mutant

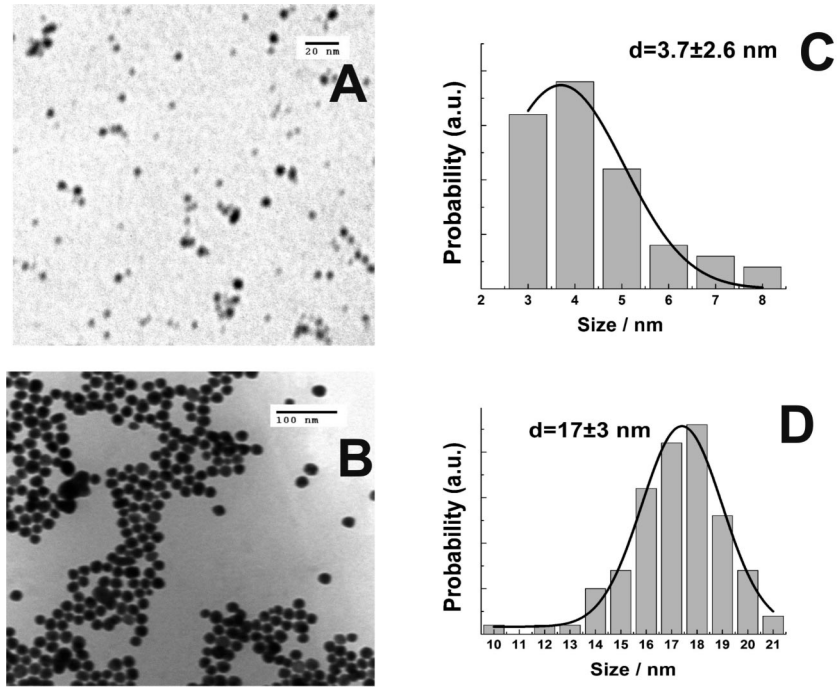

Figure 3. Representative TEM images of the gold nanoparticles used in the experiment. (A) TEM image of small nanoparticles. (B) TEM image of large nanoparticles The size histograms indicating the average size and size distribution of the gold nanoparticles are shown in (C) and (D), respectively.

MspA^{cys} on the binding of gold nanoparticles is studied by luminescence spectroscopy. MspA^{cys} contains a ring of eight thiol groups within the pore that are only accessible to the smaller gold nanoparticles.

It is well-known that the photoluminescence of a fluorophore is greatly affected by the presence of a metal surface. Briefly, the presence of a metal surface affects the radiative and nonradiative rates of fluorescence and phosphorescence as well the rate of light absorption.[17] These effects are even more pronounced with metal nanoparticles when their surface plasmon resonance is close to the transition of the fluorophore. Qualitatively, the quenching of fluorescence is most significant if the fluorophore is within a few nanometers of the surface of the metal nanoparticle. For example, the effect of fluorescence quenching dominates up to a distance of approximately 5 nm from the nanoparticle surface. On the other hand, at distances between 5–20 nm, fluorescence enhancement is the dominant mechanism.

Both MspA and MspA^{cys} possess several amino acids that contribute to the total luminescence of the protein. The strongest emitting fluorophore of MspA is tryptophan.[18] The spectrum features a strong absorption band at 280 nm (Figure 4). The fluorescence emission of tryptophan is centered at around 350 nm. The quantum yield (Φ) of this primary fluorescence is known to vary between approximately $\Phi = 0.20$ and $\Phi = 0.80$, depending on protein conformation and environment.[19]

The fluorescence emissions occurring from the excitation ($\lambda = 280$ nm) of the tryptophans of MspA in the presence and absence of the small and large gold nanoparticles are summarized in Figure 5. In all cases the fluorescence emission band is centered around 350 nm. Both MspA and

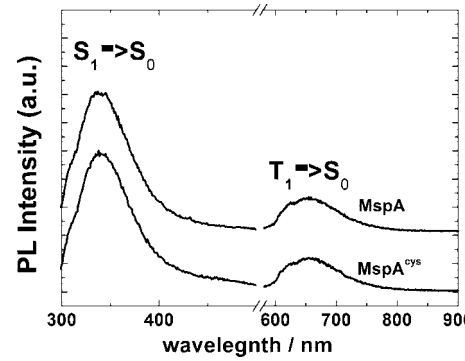

Figure 4. Fluorescence ($S_1 \rightarrow S_0$) and phosphorescence ($T_1 \rightarrow S_0$) spectra of the MspA and MspA^{cys}. The peak originates from the 32 tryptophans[8] present in the proteins. The samples are photoexcited at 280 nm.

MspA^{cys} show similar trends; however, the observed fluorescence quenching by the small gold nanoparticles is more pronounced in MspA^{cys}, whereas the fluorescence enhancement by the larger gold nanoparticles is less distinct. Note that the concentrations of MspA and of the gold particles of the same size are exactly the same, permitting us to draw direct comparisons of their photophysical behavior. The absorption cross section of the large nanoparticle is greatly increased, which could cause large self-absorption effects, making the comparison of the protein and Au@MspA complexes difficult. Therefore, the concentration of the large gold nanoparticles is chosen to be significantly smaller than that of the small gold nanoparticles. In parts a and c of Figure 5, the fluorescence of MspA (a) and MspA^{cys} (c) by the small gold nanoparticles drops to 55 ± 20% and 24 ± 20% of its initial value, respectively. In parts b and d of Figure 5 the fluorescence enhancements (I/I_0) of MspA (b) and MspA^{cys}

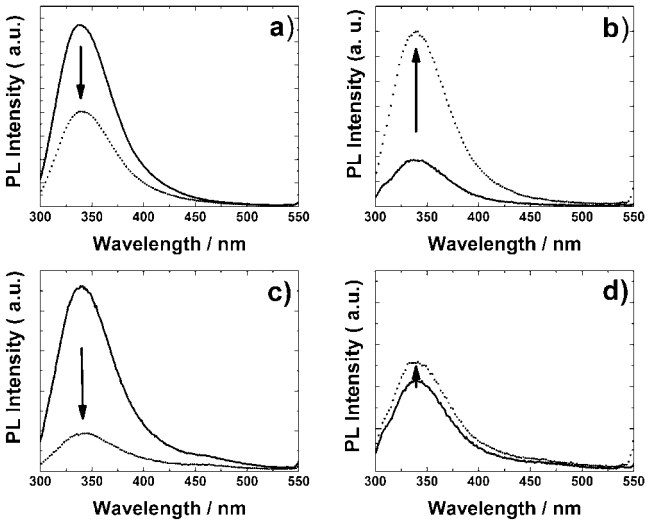

Figure 5. Fluorescence spectra of MspA before (solid line) and after (dashed line) the addition of small (a) and large (b) gold nanoparticles to the protein solution. Fluorescence spectra of $MspA^{cys}$ before (solid line) and after (dashed line) the addition of small (c) and large (d) gold nanoparticles to the protein solution. The concentration of MspA and $MspA^{cys}$ in the solution is 1.09×10^{-9} mol/L. The concentration of the small and large gold nanoparticles in solutions is 3.67×10^{-8} and 1.13×10^{-11} mol/L, respectively. The excitation wavelength is 280 nm.

(d) caused by the larger gold nanoparticles are 270 ± 20% and 130 ± 20%, respectively.

Interestingly, only freshly prepared small gold samples exhibited quenching of the fluorescence of MspA. After aging for a month, the small gold nanoparticle samples induce increased tryptophan emissions, very similar to the large gold nanoparticles. We speculate, that the cause for this effect is most likely the aging (Ostwald ripening) of the gold nanoparticles, which increases the fraction of bigger particles and consequently reduces the proportion of the very small gold particles.

A more detailed comparison of the fluorescence data is shown in Figure 6. The fluorescence spectra of the previous data (shown in Figure 5) are normalized to the peak maximum at 350 nm to observe changes in the fluorescence peak shape. Clearly discernible changes occur when assemblies between $MspA^{cys}$ and the smaller nanoparticles are formed. The spectra of the wild-type MspA before and after the addition of nanoparticles differ much less than those for $MspA^{cys}$. Interestingly, the red side of the tryptophan fluorescence is less affected. The difference spectra between the small gold $Au@MspA^{cys}$ and the $MspA^{cys}$ indicate a fluorescence peak centered at about 370 nm. On the basis of previous observations, the 370 nm peak corresponds most likely to those tryptophan molecules that can be found in a polar (aqueous) environment.[20] On the basis of this observation, the most likely location of these particular tryptophans is at position 181, which is located near the porin's "rim" and, therefore, exposed to a polar environment. In sharp contrast, no changes of the peak shapes are observed for the complexes of MspA with the larger gold nanoparticles. (Figure 6, panels b and d)).

Finally, a second photoluminescence experiment is carried out to excite the nanoparticles at a wavelength where no appreciable absorption of the MspA protein takes place. The previously described combinations of the MspA proteins and the smaller and bigger gold nanoparticle samples are shown in Figure 7. However, excitation is performed this time at 500 nm. The data presented in parts a and c of Figure 7 show that the assemblies of the small gold nanoparticles with MspA feature emission of the protein's tryptophans corresponding to the $T_1 \rightarrow S_0$ transition around $\lambda = 775$ nm

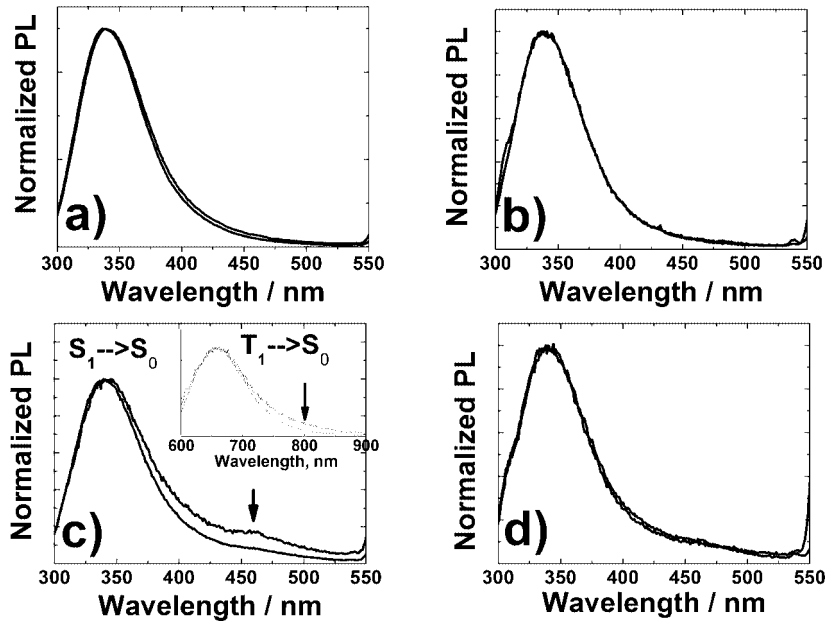

Figure 6. Same as Figure 5, but the fluorescence is normalized to the peak maximum. Panel c inset shows the $T_1 \rightarrow S_0$ transition of the $MspA^{cys}$ before (solid line) and after (dashed line) addition of small gold nanoparticles to the protein solution. The arrows indicate the position of the relative increase of fluorescence in the spectrum.

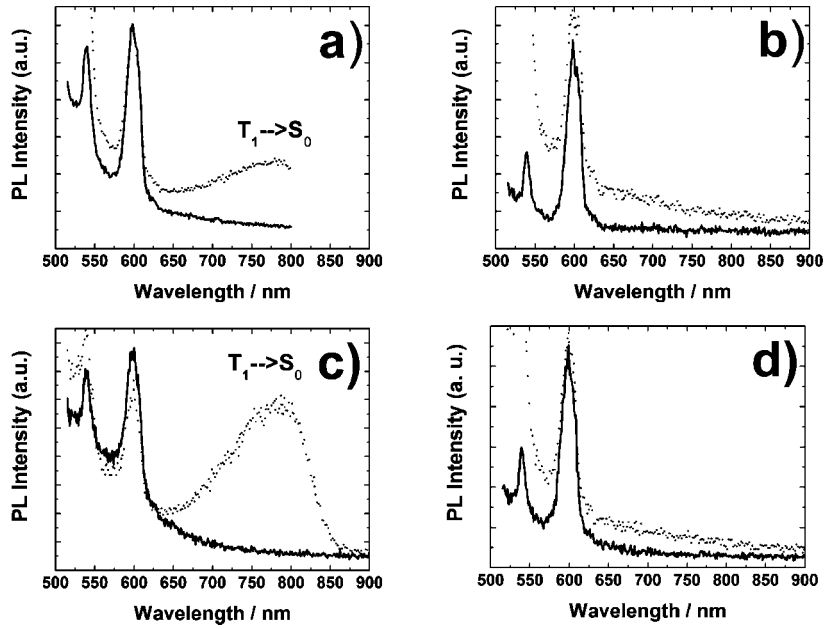

Figure 7. Photoluminescence spectra of MspA before (solid line) and after (dotted line) the addition of small (a) and large (b) gold nanoparticles to the protein solution. Photoluminescence spectra of $MspA^{cys}$ before (solid line) and after (dotted line) the addition of small (c) and large (d) gold nanoparticles to the protein solution. The concentrations of protein and nanoparticles are the same as before. The sharp features are Raman lines of the solvents. The photoluminescence of only gold nanoparticle solution (not shown) is negligible in the solution.

(phosphorescence).[20] The occurrence of phosphorescence is a strong indication that the nanoparticle and protein are indeed in close contact.[21] Interestingly, the complexes between the large gold nanoparticles and MspAs do not show the same effect. Note that the sharp features at approximately 550 and 600 nm are Raman lines of the solvents. The fluorescence of both gold nanoparticles in aqueous solution is found to be negligible.

The observed differences with respect to the occurrence of phosphorescence are due to the location of the nanoparticles attached to MspA. Whereas the smaller gold nanoparticles permit their binding within the pore of MspA, the larger nanoparticles have to be bound at the exterior of MspA due to size exclusion. The observed phosphorescence quenching of the MspA's tryptophan units can be regarded as mechanistic proof of the proximity of the excited gold NP and at least some tryptophan units within the NP@MspA assembly. On the other hand, the observed fluorescence enhancement of the excited tryptophan units in the presence of the bigger gold nanoparticles clearly suggests that some kind of binding must take place as well. In principle, fluorescence quenching could be expected if there is only a single fluorophore in the protein even in the case of a big nanoparticle, but there are 32 tryptophans present at various distances from the large gold nanoparticles since no docking takes place. In addition, the presence of large gold nanoparticles may interrupt the energy transfer network of tryptophans. Clearly, in the case of docked small gold nanoparticles, distance distribution is more symmetric relative to the metal surface. An important question is where the nanoparticles are relative to the MspA and $MspA^{cys}$. When the protein is anchored on mica, the nanoparticles are bound to the MspA from the TOP for both small and large nanoparticles.[22]

High-Performance Liquid Chromatography (HPLC) Separation of the Au@MspA Complexes. In order to estimate the binding constants between MspA and the smaller and bigger gold nanoparticles, a HPLC procedure is used that had been originally developed for the purification of MspA. In Figure 8, two typical HPLC chromatograms belonging to MspA and the supramolecular adduct of small gold nanoparticles and MspA are shown. The two peaks of MspA at 16.4 and 20.8 min occur due to hydrophobic clustering of MspA; at higher surfactant concentration, only one peak is discernible (at 16.9 min). However, we would like to compare HPLC chromatograms that have been obtained under exactly the same experimental conditions.

It is known from the HPLC purification of other MspA adducts (e.g., dihydroindolizines as optical switches[23] within the inner pore or ruthenium(II)−quaterpyridinium complexes as channel blockers[24]) that the closing of the inner MspA pore leads to a significant shift of the observed retention time. They can be found between 1.5 and 3.0 min, depending on the channel blockers used. We interpret the finding reported here as independent proof for the binding of the small and the big NPs to MspA. In both cases, the channel is blocked by either binding within (small NPs) or on top of MspA (big NPs).

The binding constants of both nanoparticles with MspA are calculated according to

$$K_B = \frac{[\mathrm{Au@MspA}]}{([\mathrm{Au}]^0 - [\mathrm{Au@MspA}])([\mathrm{MspA}]^0 - [\mathrm{Au@MspA}])} \quad (1)$$

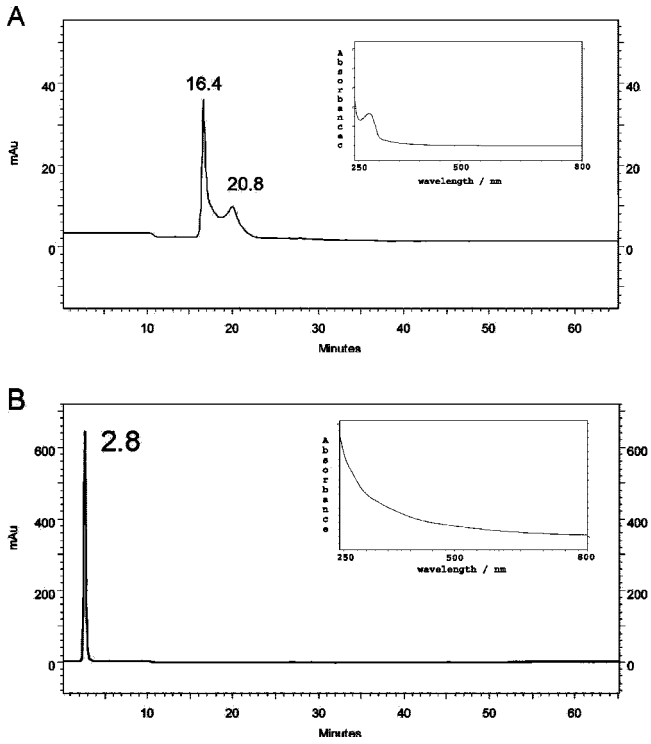

Figure 8. HPLC chromatograms of MspA (A) and small Au@MspA (B). Upon binding of the nanoparticles, the MspA peak shifts from 16.5/19.8 to 2.8 min (small Au@MspA) and 3.2 min (big Au and MspA). Note that the peak maxima of the small gold nanoparticles (1.8 min) and large gold nanoparticles (2.5 min) are distinctly different (not shown). The corresponding UV−vis spectra (shown as insets) confirmed the identity of the peaks. Principally, the same results are obtained when using $MspA^{cys}$ and MspA.

where K_B is the binding constant, [Au@MspA] is the concentration (mol/L) of the supramolecular assembly of small or big gold nanoparticles and MspA, $[MspA]^0$ is the concentration of MspA (mol/L) in the absence of NPs, and $[Au]^0$ is the starting concentration of the nanoparticles (mol/L). The results are summarized in Table 1.

It is of importance for hyperthermia experiments using either gold nanoparticles or magnetic particles featuring an outer layer of gold that the binding constants of the small gold nanoparticles are very high. We have shown that these particles are able to bind within MspA and thus form 1:1 supramolecular complexes. If $MspA^{cys}$ is used, the binding constant increases by at least 3 orders of magnitude indicating that these assemblies will be stable enough for their use within the (human) body. It is of interest as well that the binding constants between MspA and the big gold nanoparticles are distinctly higher than those of MspA and the smaller nanoparticles. We propose the possible reason for this behavior: (a) the big gold nanoparticles that are excluded from the interior of MspA can bind to the hydrophobic docking zone of MspA and (b) therefore clusters of MspA and the big gold nanoparticles are likely. However, eq 1 only describes 1:1 stoichiometry and we do not know the aggregation numbers of possible clusters. Therefore, the binding constants calculated for the big nanoparticles and MspA according to (1) are most likely high too.

Table 1. Binding Constants K_B (L/mol) Calculated from the HPLC Chromatograms Using Equation 1 and the Starting Concentrations of $[MspA]^0$ (1.09×10^{-9} mol/L) and Gold Nanoparticles $[Au]^0$: Small (3.67×10^{-8} mol/L) and Big (1.13×10^{-11} mol/L)

nanoparticle assembly	binding constant, K_B (L/mol)
small Au@MspA	1.3×10^9
large Au@MspA	2.22×10^{10}
small Au@$MspA^{cys}$	$>10^{12}$ (irreversible)[a]
large Au@$MspA^{cys}$	1.7×10^{10}

[a] No free MspA could be detected.

The interactions of two gold nanoparticles of different sizes (average diameters of 3.7 ± 2.6 and 17 ± 3 nm) with the wild type of the mycobacterial porin MspA and a tailored cysteine mutant MspA Q126C by means of fluorescence/phosphorescence spectroscopy are studied. Strong quenching of the MspA's tryptophan fluorescence is observed, indicating that the small gold nanoparticles are able to dock within the MspA pore and form supramolecular assemblies. The addition of eight cysteines within the MspA goblet by site specific mutation further increases the binding of the small gold nanoparticles within the $MspA^{cys}$ pore. Exciting the surface plasmon resonance of the small gold nanoparticles shows energy transfer to the porin, which is absent in the case of large nanoparticles. Furthermore, the difference spectra data indicate there is an interaction between the protein and the gold nanoparticles. Contrary to the behavior of the small nanoparticles, the bigger nanoparticles cannot dock within the homopore of MspA because of size exclusion. This behavior is consistent with the observed fluorescence enhancement due to energy transfer from the surface plasmon of the bigger nanoparticles to the tryptophan residues of the MspAs.

When the nanoparticles are excited directly, the observed phosphorescence enhancement of the MspA tryptophan units is additional mechanistic proof of the formation of Au@MspA assemblies. Most interestingly, the observed fluorescence enhancement of the excited tryptophan units in the presence of the bigger, directly excited, gold nanoparticles clearly suggests that some kind of binding must take place. These results are corroborated by HPLC experiments. The binding constant of the small gold nanoparticles within $MspA^{cys}$ exceeds 10^{12} (L/mol). This strongly suggests that Au@MspA assemblies, when designed correctly, are stable enough to be used as therapeutic agents.

Experimental Details. Chemicals and Porins. Hydrogen tetrachloroaurate(III) trihydrate ($HAuCl_4 \cdot 3H_2O$, 99.99%), sodium borohydride ($NaBH_4$, 98%), mercaptosuccinic acid (98%), abbreviated as MSA, methanol, *n*-octylpolyoxyethylene, and sodium citrate ($Na_3C_6H_5O_7 \cdot 2H_2O$) MspA and a mutant of MspA possessing a cysteine residue in position 126 ($MspA^{cys}$) were generous gifts from Professor Michael Niederweis, Department of Microbiology at the University of Alabama at Birmingham.

Synthesis of Gold Nanoparticles. Small gold nanoparticles were synthesized by the method described by Chen and Kimura et al.[25] Briefly, a mixture of 197 mg of $HAuCl_4$ is dissolved in 4 mL of doubly distilled water and 187.68 mg of MSA dissolved in 100 mL of methanol is prepared

under inert atmosphere. A solution of $NaBH_4$ (189.15 mg of $NaBH_4$ in 25 mL of water) is slowly added at the rate of 2 mL/min. The solution is then stirred for 1 h. Finally, a dark-brown precipitate of gold nanoparticles is formed. The gold nanoparticles are centrifuged at 8500 rpm for 10 min to obtain a residue of nanoparticles. The nanoparticles are washed twice with 20% (v/v) water/methanol mixture once with pure methanol. The large gold nanoparticles are prepared from the reduction of $HAuCl_4$ solution by sodium citrate solution as described by Turkevitch et al.[26] Briefly, 5 mg of $HAuCl_4$ and 50 mg of sodium citrate are dissolved in 95 and 5 mL of doubly distilled water, respectively. The $HAuCl_4$ solution is heated to about 70 °C, the sodium citrate solution is added, and the mixture is vigorously stirred for 50 min. The color of the solution gradually changes from faint pink to wine red. The resulting large gold nanoparticles have a size of approximately 17 ± 3 nm.

Neutron Activation Analysis of Gold Nanoparticles. The concentration of gold nanoparticles in the solution state is measured by means of neutron activation analysis (NAA). In this process, a sample and a standard sample are activated by neutrons under the same conditions. The specific activity of the samples is then measured. The activity of the samples after irradiation is directly proportional to the amount (concentration) of isotope present in the sample. The ratio of the specific activity to concentration of both samples is equal. From this relationship, and using the average nanoparticle sizes determined by the transmission electron microscopy (TEM) analysis, the concentration of gold nanoparticles in a solution is calculated.

Transmission Electron Microscopy. The sizes of the different nanoparticles are determined with TEM. This is achieved using a Philips CM-200 TEM, operating at 100 kV. A small fraction of the nanoparticle solution is diluted to one-fifth of its original volume, and a drop of the diluted solution is spread over a copper grid (300 mesh size) supporting a thin film of amorphous carbon. To reduce the damage from the electron beam, the sample is cooled to liquid nitrogen temperature during data collection.

HPLC Analysis of the Nanoparticle and MspA Complexes. The binding constants of both of the small and large gold nanoparticles bound to MspA are measured by HPLC (Shimadzu Prominence) employing a POROS HQ/20 anion exchange column and a flux of 0.50 mL min^{-1}. Two buffers are used: AOP05 (25 mM HEPES, pH 7.5, 10 mM NaCl, 0.5% OPOE) and BOP05 (25 mM HEPES, pH 7.5, 2 M NaCl, 0.5% OPOE). A typical gradient is 100% AOP05 (0–5 min), followed by a linear gradient to 100% BOP05 (5–35 min). The eluent is kept at 100% BOP05 (35–50 min). Finally, the salt concentration is returned linearly to 10 mM (100% AOP05) (50–60 min). The stop rime is set at 65 min. Peak detection is achieved using UV−vis (diode-array).

Modeling of Nanoparticle and MspA Complexes. A series of calculations are performed using the porin octamer coordinates obtained from the crystal structure of MspA (PDB code: 1UUN). First, a gold face-centered cubic lattice is constructed using the experimental Au−Au contact distance of 0.288 nm.[27] Spherical Au nanoparticles of varying diameter are then isolated from the lattice. The center of mass of each nanoparticle is then moved along the central axis of the porin corresponding to various distances (Z) from the constriction site. A complex is rejected if any Au atom is located within 0.3 nm of any porin backbone (N, C^{α}, C, O) or C^{β} atom. The distance (D) of the nearest Au atom to the C^{β} atom of the Q126 residue is then determined as a function of Z. Assuming bond lengths for the C^{β}−S and S−Au bonds of 0.182 and 0.24 nm, respectively, together with a C^{β}−S−Au bond angle of 100°[28] suggests an optimal C^{β}−Au distance of 0.33 nm for the formation of S−Au covalent bonds.

Acknowledgment. The authors thank Professor Michael Niederweis, Department of Microbiology of the University of Alabama at Birmingham for the gift of MspA and its cysteine mutant. This research has been made possible by Grant Number P20 RR015563 from the National Center for Research Resources, a component of the National Institutes of Health, and the State of Kansas. Its contents are solely the responsibility of the authors and do not necessarily represent the official view of the NCRR or NIH. V.C. and S.H.B. also thank the Terry C. Johnson Center for Basic Cancer Research at KSU for financial support.

References

(1) Pissuwan, D.; Cortie, C. H.; Valenzuela, S. M.; Cortie, M. B. *Gold Bull.* **2007**, *40*, 121–129.
(2) Qu, X.; Norbert, K.; Li, Z.; Wang, J.; Zhang, Z.; Huettmann, G. Confocal, Multiphoton, and Nonlinear Microscopic Imaging III. *Proc. SPIE−Int. Soc. Opt. Eng.* **2007**, *6630*, 66301C/1–66301C/8.
(3) Polsky, R.; Gill, R.; Kaganovsky, L.; Willner, I. *Anal. Chem.* **2006**, *78*, 2268–2271.
(4) Pavlov, V.; Xiao, Y.; Shlyahovsky, B.; Willner, I. *J. Am. Chem. Soc.* **2004**, *126*, 11768–11769.
(5) Willner, I.; Baron, R.; Willner, B. *Biosens. Bioelectron.* **2007**, *22*, 1841–1852.
(6) Wagner, E. *Expert Opin. Biol. Ther.* **2007**, *7*, 587–593.
(7) Katz, E.; Willner, I. *Angew. Chem., Int. Ed.* **2004**, *43* (45), 6042–6108.
(8) Mukherjee, P.; Ahmad, A.; Mandal, D.; Senapati, S.; Sainkar, S. R.; Khan, M. I.; Parishcha, R.; Ajaykumar, P. V.; Alam, M.; Kumar, R.; Sastry, M. *Nano Lett.* **2001**, *1* (10), 515–519.
(9) Niemeyer, C. M. *Angew. Chem., Int. Ed.* **2001**, *40* (22), 4128–4158.
(10) Engelhardt, H.; Gerbl-Rieger, S.; Krezmar, D.; Schneider-Voss, S.; Engel, A.; Baumeister, W. *J. Struct. Biol.* **1990**, *105*, 92–102.
(11) Faller, M.; Niederweis, M.; Schulz, G. E. *Science* **2004**, *303*, 1189–1192.
(12) Nie, S.; Xing, Y.; Kim, G. J.; Simons, J. W. *Annu. Rev. Biomed. Eng.* **2007**, *9*, 257–288.
(13) Cavaliere, R.; Ciocatto, E. C.; Giovanella, B. C.; Heidelburger, C.; Jonson, R. O.; Margottini, M.; Mondovi, B.; Moricca, B. C.; Rossi-Fanelli, A. *Cancer* **1967**, *20*, 1351–1384.
(14) Orgill, D. P.; Porter, S. A.; Taylor, H. O. *Ann. N.Y. Acad. Sci.* **2005**, *1066*, 106–118.
(15) http://info.tuwien.ac.at/iflt/safety/section1/1_1_1.htm.
(16) http://omlc.ogi.edu/spectra/aorta/index.html.
(17) Lakowicz, J. R. *Anal. Biochem.* **2001**, *298* (1), 1–24.
(18) Heinz, C.; Engelhardt, H.; Niederweis, M. *J. Biol. Chem.* **2003**, *278*, 10.
(19) Papp, S.; Vanderkooi, J. M. *Photochem. Photobiol.* **1989**, *49*, 775–84.
(20) Stephan, J.; Stemmer, V.; Niederweis, M. Consecutive gene deletions in *Mycobacterium smegmatis* using the yeast FLP recombinase. *Gene* **2004**, *343*, 181–190.

(21) Chen, Y.; Barkley, M. D. *Biochemistry* **1998**, *37* (28), 9976–9982.
(22) Basel1, Matthew T.; Dani, Raj Kumar; Kang, Myungshim; Pavlenok, Mikhail; Chikan, Viktor; Smith, Paul E.; Niederweis, Michael; Bossmann, Stefan H. *Angew. Chem.*. Submitted for publication.
(23) Shrestha, T.; Kalita, M.; Sukumaran, S.; Niederweis, M.; Bossmann, S. H. *42nd Midwest Regional Meeting of the American Chemical Society*, 2007.
(24) Gamage, P., Kalita, M.; Bossmann, S. H. To be published.
(25) Chen, S. H.; Kimura, K. *Langmuir* **1999**, *15* (4), 1075–1082.
(26) Turkevich, J.; Stevenson, P. C.; Hillier, J. *Discuss. Faraday Soc.* **1951**, (11), 55.
(27) De, G. T.; Rao, C. N. R. *J. Mater. Chem.* **2005**, *15* (8), 891–894.
(28) Rai, B.; Sathish, P.; Malhotra, C. P.; Pradip; Ayappa, K. G *Langmuir* **2004**, *20* (8), 3138–3144.

NL072658H